Physics Letters B 734 (2014) 286–289

Contents lists available at ScienceDirect

Physics Letters B

www.elsevier.com/locate/physletb

LHC jet suppression of light and heavy flavor observables

Magdalena Djordjevic [a,*], Marko Djordjevic [b]

[a] Institute of Physics Belgrade, University of Belgrade, Serbia
[b] Faculty of Biology, University of Belgrade, Serbia

ARTICLE INFO

Article history:
Received 14 January 2014
Received in revised form 16 May 2014
Accepted 16 May 2014
Available online 21 May 2014
Editor: W. Haxton

ABSTRACT

Jet suppression of light and heavy flavor observables is considered to be an excellent tool to study the properties of QCD matter created in ultra-relativistic heavy ion collisions. We calculate the suppression patterns of light hadrons, D mesons, non-photonic single electrons and non-prompt J/ψ in Pb + Pb collisions at the LHC. We use a theoretical formalism that takes into account finite size *dynamical* QCD medium with finite magnetic mass effects and running coupling, which is integrated into a numerical procedure that uses no free parameters in model testing. We obtain a good agreement with the experimental results across different experiments/particle species. Our results show that the developed theoretical formalism can robustly explain suppression data in ultra relativistic heavy ion collisions, which strongly suggests that pQCD in Quark–Gluon Plasma is able to provide a reasonable description of the underlying jet physics at LHC.

1. Introduction

A major goal of RHIC and LHC experiments is to understand properties of a QCD medium created in ultra-relativistic heavy ion collisions. A powerful tool to map the properties of such a medium is to compare high-p_t hadron suppression [1] measurements with the corresponding theoretical predictions [2–6]. Such predictions require accurate computations of jet energy loss, since the suppression is the consequence of the energy loss of high energy partons that move through the plasma [7–10]. In [11,12], we developed a theoretical formalism for the calculation of the first order in opacity radiative energy loss in a realistic finite size dynamical QCD medium, which we subsequently generalized to the case of finite magnetic mass in [13]. These studies, together with the calculations of the collisional energy loss in a finite size QCD medium that we previously developed [14], provide reliable framework for energy loss computation in Quark–Gluon Plasma (QGP).[1]

We here extend this formalism to running coupling and integrate it in a numerical procedure that can generate state-of-the-art predictions for LHC experimental measurements. The numerical procedure includes multi-gluon fluctuations [16] (see also [19]), path length fluctuations [20] and most up-to-date jet production [21,22] and fragmentation functions [23]. Our strategy is to generate predictions for a diverse set of experimental probes, for which experimental data are available at LHC, in order to comprehensively test our understanding of QCD matter created in these collisions. Specifically, we will generate suppression predictions for light hadrons, D mesons, non-photonic single electrons and non-prompt J/ψ in most central 2.76 TeV Pb + Pb collisions at the LHC. These predictions will be generated under the same numerical framework, by using the same set of parameters and with no free parameters used in model testing. Since the previous studies provide comparisons for a substantially smaller set of observables (see e.g. [24]), with free parameters commonly used, the comprehensive comparison of our predictions with the experimental measurements will allow testing to what extent pQCD calculations in QGP can explain the underlying high-p_t hadron physics at corresponding LHC experiments.

2. Theoretical framework

2.1. General framework

We use the generic pQCD convolution in order to calculate the quenched spectra of partons, hadrons, electrons and J/ψ:

$$\frac{E_f d^3\sigma}{dp_f^3} = \frac{E_i d^3\sigma(Q)}{dp_i^3} \otimes P(E_i \to E_f) \otimes D(Q \to H_Q) \otimes f(H_Q \to e, J/\psi). \quad (1)$$

* Corresponding author.

[1] Our energy loss formalism presents an extension of a well known DGLV [15] energy loss to the case of finite size dynamical QCD medium, and consequently includes LPM effect in the regime of a thin/dilute media. Note that the LPM effect in the regime of thick/dense media is included in [17,18].

http://dx.doi.org/10.1016/j.physletb.2014.05.053

In the equation above subscripts "i" and "f" correspond, respectively, to "initial" and "final", Q denotes quarks and gluons, while the terms in the equation correspond to the following:

(i) $E_i d^3\sigma(Q)/dp_i^3$ denotes the initial quark spectrum, which are extracted from [21,25] for charm and bottom quarks and from [22] for gluons and light quarks.
(ii) $P(E_i \to E_f)$ is the energy loss probability, which is generalized to include both radiative and collisional energy loss in a realistic finite size dynamical QCD medium, as well as multi-gluon [16] fluctuations (see also [19]), path-length fluctuations [20], running coupling and finite magnetic mass.[2]
(iii) $D(Q \to H_Q)$ is the fragmentation function of quark or gluon Q to hadron H_Q, where for light hadrons, D mesons and B mesons we use, respectively, DSS [23], BCFY [26] and KLP [27] fragmentation functions.
(iv) For heavy quarks, we also have the decay of hadron H_Q into single electrons or J/ψ, which is represented by the functions $f(H_Q \to e, J/\psi)$. The decays of D, B mesons to non-photonic single electrons, and decays of B mesons to non-prompt J/ψ are obtained according to [21].

Note that Eq. (1) represents that, in our calculations, the four steps outlined above are treated separately and in the order defined by this expression.

Furthermore, in the calculations of jet suppression, we use the following assumptions:

(i) The final quenched energy E_f is sufficiently large, so that we can employ the eikonal approximation.
(ii) The jet to hadron fragmentation functions are the same for e^+e^- and Pb + Pb collisions, which is expected to be valid in a deconfined QCD medium.
(iii) We can separately treat radiative and collisional energy loss, so that we first calculate how quark and gluon spectra change due to radiative energy loss, and then due to collisional energy loss. This approximation is reasonable as long as the radiative and collisional energy losses are sufficiently small (as assumed by soft-gluon, soft-rescattering approximation, which is employed in all energy loss calculations so far), and when collisional and radiative energy loss processes are decoupled from each other (as follows from HTL approach [28] that is used in our energy loss calculations [11,12,14,13]).
(iv) We can independently treat multiple emissions in multi-gluon fluctuations, which is a reasonable assumption [29] within (the above mentioned) soft-gluon approximation.

2.2. Path-length and multi-gluon fluctuations

Multi-gluon fluctuations take into account that the energy loss is a distribution, while path-length fluctuations take into account that particles traverse different paths in the QCD medium. Path length fluctuations are included in the energy loss probability according to [20] (see also [30]):

$$P(E_i \to E_f = E_i - \Delta_{rad} - \Delta_{coll}) = \int dL\, P(L) P_{rad}(\Delta_{rad}; L) \otimes P_{coll}(\Delta_{coll}; L). \tag{2}$$

In the above expression, $P(L)$ is the path-length distribution. For 0–5% most central collisions, we used the distribution from [31]. Note that path-length distribution is the same for all jet varieties, since it corresponds to a geometric quantity.

Numerical method for including multi-gluon fluctuations in the radiative energy loss probability is presented in Refs. [32,33]. We recently generalized the procedure [34] to include the radiative energy loss in a finite size dynamical QCD medium [11,12], as well as finite magnetic mass effects [13]. Specifically, in accordance with [13], the gluon radiation spectrum is extracted from

$$\frac{dN_{rad}}{dx} = \frac{2C_R C_2(G) T L}{x} \int \frac{d^2k}{\pi} \frac{d^2q}{\pi} \frac{\mu_E^2 \alpha_S^2}{\pi} \frac{1 - \mu_M^2/\mu_E^2}{(\boldsymbol{q}^2 + \mu_M^2)(\boldsymbol{q}^2 + \mu_E^2)} \times \left(1 - \frac{\sin \frac{(\boldsymbol{k}+\boldsymbol{q})^2+\chi}{xE^+} L}{\frac{(\boldsymbol{k}+\boldsymbol{q})^2+\chi}{xE^+} L}\right) \frac{(\boldsymbol{k}+\boldsymbol{q})}{(\boldsymbol{k}+\boldsymbol{q})^2 + \chi} \times \left(\frac{(\boldsymbol{k}+\boldsymbol{q})}{(\boldsymbol{k}+\boldsymbol{q})^2 + \chi} - \frac{\boldsymbol{k}}{\boldsymbol{k}^2 + \chi}\right). \tag{3}$$

In the above expression E is initial jet energy, L is the length of the finite size dynamical QCD medium and T is the temperature of the medium. α_S is coupling constant, $C_R = \frac{4}{3}$ and $C_2(G) = 3$. μ_E is electric screening (the Debye mass), and μ_M is magnetic screening. $\boldsymbol{k}$ and $\boldsymbol{q}$ are transverse momenta of radiated and exchanged (virtual) gluon, respectively. $\chi \equiv M^2x^2 + m_g^2$, where x is the longitudinal momentum fraction of the heavy quark carried away by the emitted gluon, and $m_g = \mu_E/\sqrt{2}$ is the effective mass for gluons with hard momenta $k \gtrsim T$ [39].

For collisional energy loss, we approximate the full fluctuation spectrum by a Gaussian with a mean determined by the average energy loss and the variance determined by $\sigma_{coll}^2 = 2T\langle \Delta E^{coll}(E_i, L)\rangle$ [35,20]; here, $\Delta E^{coll}(E_i, L)$ is extracted from Eq. (14) in [14], while T, E_i and L are, respectively, the temperature of the medium, the initial jet energy and the length of the medium traveled by the jet.

2.3. Running coupling

We further extend this formalism by introducing the running coupling in the following way: In the radiative energy loss case, the coupling appears through the term $\mu_E^2\alpha_S^2$ (see Eq. (3) above). Starting from this expression, we here introduce the running coupling phenomenologically, since no exact calculations exist on this problem. To that end, we take that $\mu_E^2\alpha_S^2$ can be factorized as $\mu_E^2\alpha_S(Q_v^2)\alpha_S(Q_k^2)$, where the first α_S corresponds to the interaction between the jet and the virtual (exchanged) gluon, while the second α_S corresponds to the interaction between the jet and the radiated gluon (see [11]).[3] The Debye mass μ_E can be obtained by self-consistently solving the following equation [36]:

$$\frac{\mu_E^2}{\Lambda_{\rm QCD}^2} \ln\left(\frac{\mu_E^2}{\Lambda_{\rm QCD}^2}\right) = \frac{1 + n_f/6}{11 - 2/3n_f} \left(\frac{4\pi T}{\Lambda_{\rm QCD}}\right)^2, \tag{4}$$

where $\Lambda_{\rm QCD}$ is perturbative QCD scale, and n_f is number of the effective degrees of freedom. Note that, in our calculation, μ_E does not run, but is a constant determined by the above equation.

Running coupling $\alpha_S(Q^2)$ is defined as in [37]:

$$\alpha_S(Q^2) = \frac{4\pi}{(11 - 2/3n_f)\ln(Q^2/\Lambda_{\rm QCD}^2)}. \tag{5}$$

[2] Detailed discussion on the jet energy loss generalization to the case of finite magnetic mass is provided in [13]. Note that the finite magnetic mass is introduced phenomenologically (though consistently) in the energy loss, since HTL approach that we use in the calculations requires zero magnetic mass.

[3] Note that, in this factorization we take the same structure as in the representative diagram for the radiative energy loss (i.e. the diagram where interaction of the jet with the medium is followed by gluon radiation).

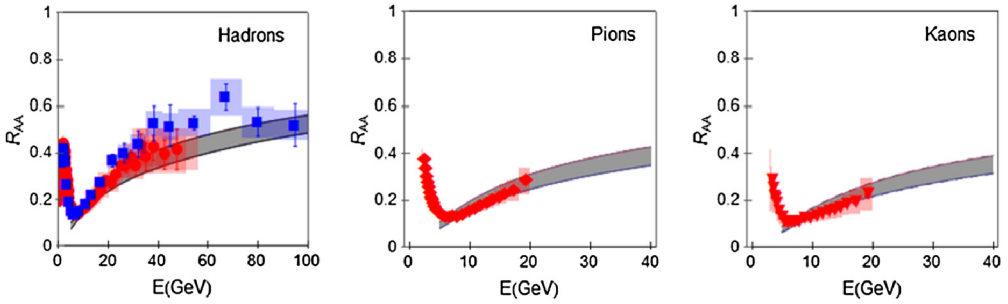

Fig. 1. *Theory vs. experimental data for momentum dependence of light flavor R_{AA}.* The left panel shows the comparison of light hadron suppression predictions with experimentally measured R_{AA} for charged particles. Red circles and blue squares, respectively, correspond to ALICE [47] and CMS [49] experimental data. The central panel shows the comparison of pion suppression predictions with preliminary $\pi^{\pm}$ ALICE [48] R_{AA} data (red rhomboids), while the right panel shows the comparison of kaon suppression predictions with preliminary $K^{\pm}$ R_{AA} ALICE data [48] (red triangles). All the data correspond to 0–5% central 2.76 TeV Pb + Pb collisions. On each panel, the gray region corresponds to the case where $0.4 < \mu_M/\mu_E < 0.6$, with the upper (lower) boundary of each band that corresponds to $\mu_M/\mu_E = 0.4$ ($\mu_M/\mu_E = 0.6$). (For interpretation of the references to color in this figure legend, the reader is referred to the web version of this article.)

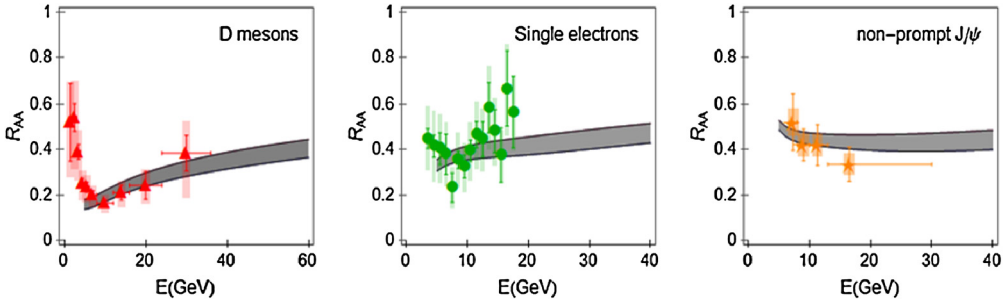

Fig. 2. *Theory vs. experimental data for momentum dependence of heavy flavor R_{AA}.* The left panel shows the comparison of D meson suppression predictions with D meson R_{AA} ALICE preliminary data [50] (red triangles) in 0–7.5% central 2.76 TeV Pb + Pb collisions. The central panel shows the comparison of non-photonic single electron suppression predictions with the corresponding ALICE preliminary data [51] (green circles) in 0–10% central 2.76 TeV Pb + Pb collisions. The right panel shows the comparison of J/ψ suppression predictions with the preliminary non-prompt J/ψ R_{AA} CMS data [52] (orange stars) in 0–100% 2.76 TeV Pb + Pb collisions. The gray region on each panel is as defined in Fig. 1. (For interpretation of the references to color in this figure legend, the reader is referred to the web version of this article.)

To obtain $\alpha_S(Q_v^2)$, note that $Q_v^2 = ET$ [38], where E is the energy of the jet. Similarly, to obtain $\alpha_S(Q_k^2)$, note that Q_k^2 is off-shellness [37] of the jet prior to the gluon radiation and is equal to $Q_k^2 = \frac{\boldsymbol{k}^2 + M^2x^2 + m_g^2}{x}$ [11], where $\boldsymbol{k}$ is transverse momentum of the radiated gluon, M is the jet mass, x is the longitudinal momentum fraction of the jet carried away by the emitted gluon, and $m_g = \mu_E/\sqrt{2}$ is the effective mass for gluons with hard momenta $k \gtrsim T$ [39]. Note that, as introduced above, $\alpha_S(Q_{k,v}^2)$ are infrared safe (and moreover of a moderate value), so there is no need to introduce a cut-off in $\alpha_S(Q^2)$, as is usually done with running coupling elsewhere (see e.g. [40,41]).

For the collisional energy loss, the coupling appears through the term α_S^2 [14], which can be factorized as $\alpha_S(\mu_E^2)\alpha_S(Q_v^2)$ [38], with $\alpha_S(Q^2)$ given by Eq. (5).

3. Numerical results

We here show our suppression predictions for light and heavy flavor observables in central 2.76 TeV Pb + Pb collisions at LHC. The following parameters are used in the numerical calculations: QGP with effective light quark flavors $n_f = 3$ and perturbative QCD scale of $\Lambda_{\rm QCD} = 0.2$ GeV. We estimate the average temperature of QGP to be $T = 304$ MeV (the effective temperature extracted by ALICE [42]). The light quark mass is assumed to be dominated by the thermal mass $M = \mu_E/\sqrt{6}$, where Debye mass $\mu_E \approx 0.9$ GeV is obtained by self-consistently solving Eq. (4). The value for magnetic to electric mass ratio μ_M/μ_E is extracted from several independent non-perturbative QCD calculations [43–46] to be in the range $0.4 < \mu_M/\mu_E < 0.6$. The gluon mass is $m_g = \mu_E/\sqrt{2}$ [39], while the charm and the bottom mass are, respectively, $M = 1.2$ GeV and $M = 4.75$ GeV. Path-length distribution, parton production, fragmentation functions and decays, which are used in the numerical calculations, are specified in the previous section.

Fig. 1 shows momentum dependence of R_{AA} for light flavor observables, i.e. charged hadrons, pions and kaons at LHC. The predictions are compared with the relevant ALICE [47,48] and CMS [49] experimental data in central 2.76 TeV Pb + Pb collisions at LHC. Fig. 2 shows momentum dependence of R_{AA} for heavy flavor observables, i.e. D mesons, non-photonic single electrons and non-prompt J/ψ at LHC; here, the predictions are also compared with the corresponding ALICE [51,50] and CMS [52] experimental data at 2.76 TeV Pb + Pb collisions at LHC.

For all six observables shown in Figs. 1 and 2, we see a very good agreement between the predictions and the experimental data. The left panel in Fig. 1 (charged hadrons) shows an excellent agreement with ALICE data [47] (the red circles), and a somewhat worse agreement with CMS data [49] (the blue squares), since CMS charged hadron R_{AA} is systematically somewhat above the corresponding ALICE R_{AA}. Both the central and the right panel show excellent agreement between the theoretical predictions and preliminary ALICE pion and kaon R_{AA} data [48]; note that these predictions reproduce a fine qualitative resolution between pion and kaon R_{AA} data, i.e. the fact that observed kaon suppression is systematically somewhat larger compared to the pion suppression. For the heavy flavor measurements, predictions for D meson data (the left panel in Fig. 2) show a similarly good agreement with the available experimental ALICE preliminary data [50]. Though the preliminary non-photonic single electron data [51] are quite noisy

(the central panel in Fig. 2), there is a very good agreement with the corresponding theoretical predictions; further reduction of the error bars is needed for a clearer comparison. Finally, we also see a good agreement between the theoretical predictions and CMS preliminary non-prompt J/ψ data [52] (the right panel in Fig. 2), except for the last data point, for which the error bars are very large.[4]

4. Conclusions

A major theoretical goal in relativistic heavy ion physics is to develop a theoretical framework that is able to consistently explain both light and heavy flavor experimental data. We here presented suppression calculations for light and heavy flavor observables, by taking into account finite size dynamical QCD medium with magnetic mass effects and running coupling taken into account. We generated comprehensive predictions for central collisions at LHC, which include six independent observables, i.e. light hadrons, D mesons, non-photonic single electrons and non-prompt J/ψ, for which experimental measurements at LHC are available. To our knowledge, suppression predictions for such a diverse set of probes, generated by the same theory, within the same numerical procedure/parameter set, were not available before. Furthermore, no free parameters were used in the model testing, i.e. the parameter values were fixed in advance according to the literature values. Comparing these predictions with the available experimental data shows a robust agreement across the whole set of probes. Such agreement, together with our previous study addressing the heavy flavor puzzle at RHIC [34], indicates that the developed theoretical formalism can realistically model the QCD matter created in ultra-relativistic heavy ion collisions.

Acknowledgements

This work is supported by Marie Curie International Reintegration Grants within the European Commission 7th Framework Programme (PIRG08-GA-2010-276913 and PIRG08-GA-2010-276996) and by the Ministry of Science and Technological Development of the Republic of Serbia, under projects Nos. ON171004 and ON173052 and by L'OREAL–UNESCO For Women in Science Award in Serbia. We thank I. Vitev and Z. Kang for providing the initial light flavor distributions and useful discussions. We also thank M. Cacciari for useful discussion on heavy flavor production and decay processes. We thank ALICE Collaboration for providing the shown preliminary data, and M. Stratmann and Z. Kang for their help with DSS fragmentation functions.

References

[1] J.D. Bjorken, FERMILAB-PUB-82/59-THY.
[2] M. Gyulassy, Lect. Notes Phys. 583 (2002) 37.
[3] D. d'Enterria, B. Betz, Lect. Notes Phys. 785 (2010) 285.
[4] U.A. Wiedemann, Nucl. Phys. A 904–905 (2013) 3c.
[5] N. Armesto, M. Cacciari, A. Dainese, C.A. Salgado, U.A. Wiedemann, Phys. Lett. B 637 (2006) 362.
[6] G.Y. Qin, A. Majumder, Phys. Rev. Lett. 105 (2010) 262301.
[7] M. Guylassy, I. Vitev, X.N. Wang, B.W. Zhang, in: Quark Gluon Plasma 3, World Scientific, Singapore, 2003, p. 123.
[8] R. Baier, Yu.L. Dokshitzer, A.J. Mueller, D. Schiff, Phys. Rev. C 58 (1998) 1706.
[9] R. Baier, D. Schiff, B.G. Zakharov, Annu. Rev. Nucl. Part. Sci. 50 (2000) 37.
[10] A. Kovner, U.A. Wiedemann, in: Quark Gluon Plasma 3, World Scientific, Singapore, 2003, p. 192.
[11] M. Djordjevic, Phys. Rev. C 80 (2009) 064909.
[12] M. Djordjevic, U. Heinz, Phys. Rev. Lett. 101 (2008) 022302.
[13] M. Djordjevic, M. Djordjevic, Phys. Lett. B 709 (2012) 229.
[14] M. Djordjevic, Phys. Rev. C 74 (2006) 064907.
[15] M. Gyulassy, P. Levai, I. Vitev, Nucl. Phys. B 594 (2001) 371; M. Djordjevic, M. Gyulassy, Nucl. Phys. A 733 (2004) 265.
[16] M. Gyulassy, P. Levai, I. Vitev, Phys. Lett. B 538 (2002) 282.
[17] P. Arnold, G.D. Moore, L.G. Yaffe, J. High Energy Phys. 0111 (2001) 057; P. Arnold, G.D. Moore, L.G. Yaffe, J. High Energy Phys. 0206 (2002) 030; P. Arnold, G.D. Moore, L.G. Yaffe, J. High Energy Phys. 0301 (2003) 030.
[18] S. Caron-Huot, C. Gale, Phys. Rev. C 82 (2010) 064902.
[19] R. Baier, Yu.L. Dokshitzer, A.J. Mueller, D. Schiff, J. High Energy Phys. 0109 (2001) 033.
[20] S. Wicks, W. Horowitz, M. Djordjevic, M. Gyulassy, Nucl. Phys. A 784 (2007) 426.
[21] M. Cacciari, S. Frixione, N. Houdeau, M.L. Mangano, P. Nason, G. Ridolfi, J. High Energy Phys. 1210 (2012) 137.
[22] Z.B. Kang, I. Vitev, H. Xing, Phys. Lett. B 718 (2012) 482; R. Sharma, I. Vitev, B.W. Zhang, Phys. Rev. C 80 (2009) 054902.
[23] D. de Florian, R. Sassot, M. Stratmann, Phys. Rev. D 75 (2007) 114010.
[24] B. Abelev, et al., ALICE Collaboration, J. High Energy Phys. 1209 (2012) 112.
[25] M. Cacciari, M. Greco, P. Nason, J. High Energy Phys. 9805 (1998) 007; M. Cacciari, S. Frixione, P. Nason, J. High Energy Phys. 0103 (2001) 006.
[26] M. Cacciari, P. Nason, J. High Energy Phys. 0309 (2003) 006; E. Braaten, K.-M. Cheung, S. Fleming, T.C. Yuan, Phys. Rev. D 51 (1995) 4819.
[27] V.G. Kartvelishvili, A.K. Likhoded, V.A. Petrov, Phys. Lett. B 78 (1978) 615.
[28] M. Djordjevic, Nucl. Phys. A 783 (2007) 197.
[29] J.P. Blaizot, F. Dominguez, E. Iancu, Y. Mehtar-Tani, J. High Energy Phys. 1301 (2013) 143.
[30] J. Xu, A. Buzzatti, M. Gyulassy, arXiv:1402.2956.
[31] A. Dainese, Eur. Phys. J. C 33 (2004) 495.
[32] M. Djordjevic, M. Gyulassy, S. Wicks, Phys. Rev. Lett. 94 (2005) 112301.
[33] M. Djordjevic, M. Gyulassy, R. Vogt, S. Wicks, Phys. Lett. B 632 (2006) 81.
[34] M. Djordjevic, Phys. Rev. C 85 (2012) 034904.
[35] G.D. Moore, D. Teaney, Phys. Rev. C 71 (2005) 064904.
[36] A. Peshier, arXiv:hep-ph/0601119, 2006.
[37] R. Field, Applications of Perturbative QCD, Perseus Books, Cambridge, MA, 1995.
[38] S. Peigne, A. Peshier, Phys. Rev. D 77 (2008) 114017.
[39] M. Djordjevic, M. Gyulassy, Phys. Rev. C 68 (2003) 034914.
[40] B.G. Zakharov, JETP Lett. 88 (2008) 781.
[41] A. Buzzatti, M. Gyulassy, Nucl. Phys. A 904–905 (2013) 779c.
[42] M. Wilde, ALICE Collaboration, Nucl. Phys. A 904–905 (2013) 573c.
[43] Yu. Maezawa, et al., WHOT-QCD Collaboration, Phys. Rev. D 81 (2010) 091501; Yu. Maezawa, et al., WHOT-QCD Collaboration, PoS Lattice 194 (2008).
[44] A. Nakamura, T. Saito, S. Sakai, Phys. Rev. D 69 (2004) 014506.
[45] A. Hart, M. Laine, O. Philipsen, Nucl. Phys. B 586 (2000) 443.
[46] D. Bak, A. Karch, L.G. Yaffe, J. High Energy Phys. 0708 (2007) 049.
[47] K. Aamodt, et al., ALICE Collaboration, Phys. Lett. B 720 (2013) 52.
[48] A.O. Velasquez, ALICE Collaboration, Nucl. Phys. A 904–905 (2013) 763c.
[49] S. Chatrchyan, et al., CMS Collaboration, Eur. Phys. J. C 72 (2012) 1945.
[50] A. Grelli, ALICE Collaboration, Nucl. Phys. A 904–905 (2013) 635c.
[51] S. Sakai, ALICE Collaboration, Nucl. Phys. A 904–905 (2013) 661c.
[52] J. Mihee, CMS Collaboration, Nucl. Phys. A 904–905 (2013) 657c.

[4] Our J/ψ predictions are compared with the available 0–100% centrality measurements; the change in the centrality is expected to increase the suppression compared to the results presented here, though based on [52], we expect that the increase will not be significant.